



<https://openaccess.leidenuniv.nl>

### **License: Article 25fa pilot End User Agreement**

This publication is distributed under the terms of Article 25fa of the Dutch Copyright Act (Auteurswet) with explicit consent by the author. Dutch law entitles the maker of a short scientific work funded either wholly or partially by Dutch public funds to make that work publicly available for no consideration following a reasonable period of time after the work was first published, provided that clear reference is made to the source of the first publication of the work.

This publication is distributed under The Association of Universities in the Netherlands (VSNU) 'Article 25fa implementation' pilot project. In this pilot research outputs of researchers employed by Dutch Universities that comply with the legal requirements of Article 25fa of the Dutch Copyright Act are distributed online and free of cost or other barriers in institutional repositories. Research outputs are distributed six months after their first online publication in the original published version and with proper attribution to the source of the original publication.

You are permitted to download and use the publication for personal purposes. All rights remain with the author(s) and/or copyrights owner(s) of this work. Any use of the publication other than authorised under this licence or copyright law is prohibited.

If you believe that digital publication of certain material infringes any of your rights or (privacy) interests, please let the Library know, stating your reasons. In case of a legitimate complaint, the Library will make the material inaccessible and/or remove it from the website. Please contact the Library through email: [OpenAccess@library.leidenuniv.nl](mailto:OpenAccess@library.leidenuniv.nl)

### **Article details**

Sun W., Wen Y., Thiramanas R., Chen M., Han J., Gong N., Wagner M., Jiang S., Meijer M.S., Bonnet S., Butt H.J., Mailaender V., Liang X.J. & Wu S. (2018), Red-Light-Controlled Release of Drug-Ru Complex Conjugates from Metallopolymer Micelles for Phototherapy in Hypoxic Tumor Environments, *Advanced Functional Materials* 28(39): 1804227.  
Doi: 10.1002/adfm.201804227

# Red-Light-Controlled Release of Drug–Ru Complex Conjugates from Metallopolymer Micelles for Phototherapy in Hypoxic Tumor Environments

Wen Sun, Yan Wen, Rawewan Thiramanas, Mingjia Chen, Jianxiong Han, Ningqiang Gong, Manfred Wagner, Shuai Jiang, Michael S. Meijer, Sylvestre Bonnet, Hans-Jürgen Butt, Volker Mailänder,\* Xing-Jie Liang,\* and Si Wu\*

Traditional photodynamic phototherapy is not efficient for anticancer treatment because solid tumors have a hypoxic microenvironment. The development of photoactivated chemotherapy based on photoresponsive polymers that can be activated by light in the “therapeutic window” would enable new approaches for basic research and allow for anticancer phototherapy in hypoxic conditions. This work synthesizes a novel Ru-containing block copolymer for photoactivated chemotherapy in hypoxic tumor environment. The polymer has a hydrophilic poly(ethylene glycol) block and a hydrophobic Ru-containing block, which contains red-light-cleavable (650–680 nm) drug–Ru complex conjugates. The block copolymer self-assembles into micelles, which can be efficiently taken up by cancer cells. Red light induces release of the drug–Ru complex conjugates from the micelles and this process is oxygen independent. The released conjugates inhibit tumor cell growth even in hypoxic tumor environment. Furthermore, the Ru-containing polymer for photoactivated chemotherapy in a tumor-bearing mouse model is applied. Photoactivated chemotherapy of the polymer micelles demonstrates efficient tumor growth inhibition. In addition, the polymer micelles do not cause any toxic side effects to mice during the treatment, demonstrating good biocompatibility of the system to the blood and healthy tissues. The novel red-light-responsive Ru-containing polymer provides a new platform for phototherapy against hypoxic tumors.

## 1. Introduction


The success of metal complexes such as platinum (Pt) complexes for anticancer applications encourages the development of new metallodrugs.<sup>[1–5]</sup> Recent fundamental research

and clinical trials showed that ruthenium (Ru) complexes are promising alternatives for Pt drugs.<sup>[1,2]</sup> In particular, photoactivatable Ru complexes have been proposed for anticancer phototherapy, which can increase selectivity between tumor and healthy cells.<sup>[1,2,6,7]</sup> These complexes are generally nontoxic to

Dr. W. Sun, Prof. S. Wu  
Hefei National Laboratory for Physical Sciences at the Microscale  
CAS Key Laboratory of Soft Matter Chemistry  
Anhui Key Laboratory of Optoelectronic Science and Technology  
Innovation Centre of Chemistry for Energy Materials  
Department of Polymer Science and Engineering  
University of Science and Technology of China  
Hefei 230026, China  
E-mail: siwu@ustc.edu.cn

Dr. W. Sun, R. Thiramanas, M. Chen, J. Han, Dr. M. Wagner, Dr. S. Jiang,  
Prof. H.-J. Butt, Prof. V. Mailänder, Prof. S. Wu  
Max Planck Institute for Polymer Research  
Ackermannweg 10, 55128 Mainz, Germany  
E-mail: wusi@mpip-mainz.mpg.de

Dr. W. Sun  
State Key Laboratory of Fine Chemicals  
Dalian University of Technology  
2 Linggong Road, 116024 Dalian, China

 The ORCID identification number(s) for the author(s) of this article can be found under <https://doi.org/10.1002/adfm.201804227>.

Y. Wen, N. Gong, Prof. X.-J. Liang  
CAS Center for Excellence in Nanoscience and CAS Key Laboratory  
for Biological Effects of Nanomaterials and Nanosafety  
National Center for Nanoscience and Technology  
Chinese Academy of Sciences  
100190 Beijing, China  
E-mail: liangxj@nanoctr.cn

R. Thiramanas  
National Nanotechnology Center  
National Science and Technology Development Agency  
111 Thailand Science Park, Phahonyothin Road, Khlong Nueng, Khlong  
Luang, Pathum Thani 12120, Thailand

M. S. Meijer, Prof. S. Bonnet  
Leiden Institute of Chemistry  
Leiden University Gorlaeus Laboratories  
P.O. Box 9502, 2300 RA, Leiden, the Netherlands

Prof. V. Mailänder  
III. Medical Clinic  
University Medicine of the Johannes-Gutenberg University Mainz  
Langenbeckstr. 1, 55131 Mainz, Germany  
E-mail: volker.mailaender@unimedizin-mainz.de

DOI: 10.1002/adfm.201804227

nonirradiated normal cells and become highly toxic in tumor cells via selective irradiation of tumors. Phototoxicity of Ru complexes arises from two different mechanisms. One mechanism is singlet oxygen ( $^1\text{O}_2$ ) sensitization using Ru complexes for photodynamic therapy (PDT).<sup>[8–16]</sup> The other mechanism is uncaging cytotoxic ligands or Ru species via ligand photosubstitution reactions for photoactivated chemotherapy (PACT).<sup>[17–25]</sup>

The therapeutic effects of PDT are critically dependent on the local concentration of oxygen.<sup>[26,27]</sup> Because solid tumors have a hypoxic microenvironment especially in the areas far away from the blood vessels ( $>70\ \mu\text{m}$ ),<sup>[28]</sup> PDT does not work in hypoxic tumor environment. In contrast, PACT using Ru complexes is better suited than PDT for hypoxic tumor treatment because ligand photosubstitution is oxygen independent.<sup>[29–32]</sup> Thus, PACT represents a promising approach against hypoxic tumors. We and other groups have shown photoinhibition of tumor cell growth using photoactivatable Ru complexes based on combined PDT and PACT.<sup>[8,33–37]</sup> True PACT in hypoxic cancer cells is difficult to achieve due to insufficient anticancer efficiencies of uncaged ligands and Ru species. Recently, Bonnet and co-workers reported PACT against hypoxic cancer cells in vitro using a Ru complex caged with a cytotoxic ligand.<sup>[20]</sup>

The strategy was based on photouncaging of cytotoxic ligands, which inhibited the growth of hypoxic cancer cells in vitro. The next challenge is the further development of new Ru complexes for PACT in vivo. Besides photouncaging of efficient anticancer ligands or Ru species, PACT in vivo requires that photoactivatable Ru complexes have negligible side effects to healthy tissues, can accumulate in tumor cells, and can be photoactivated in the body.<sup>[33,35]</sup> However, none of the reported photoactivatable Ru-containing materials has shown therapeutic effects for PACT in vivo. Therefore, it is a challenge to design photoactivatable Ru-containing materials for PACT in vivo.

Herein, we demonstrate the design of a red-light-responsive Ru-containing block copolymer (PEG-*b*-P(CPH-*co*-RuCHL)) for phototherapy against hypoxic tumors in vivo (Figure 1). The polymer contains a hydrophilic poly(ethylene glycol) (PEG) block. PEGylation is an efficient way to reduce non-specific protein adsorption of drug carriers and improve biocompatibility.<sup>[38–40]</sup> Importantly, the hydrophobic block of the polymer contains newly synthesized drug–Ru complex conjugates on the polymer side chains (Figure 1a). The commercial anticancer drug chlorambucil (CHL) was conjugated with the Ru complex. This novel design, for the first time, results

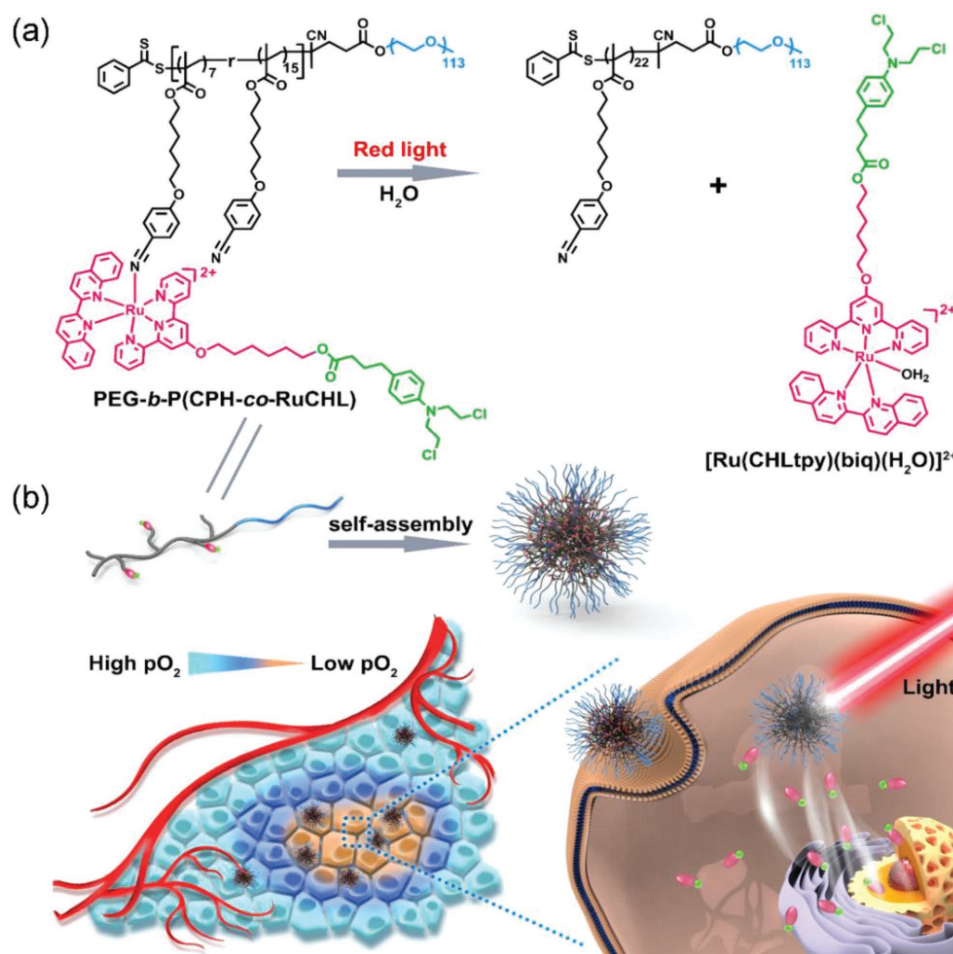


**Figure 1.** a) Structure and photoreaction of the metallopolymer PEG-*b*-P(CPH-*co*-RuCHL). The green and purple parts in the chemical structures represent the drug (CHL) moiety and the Ru complex moiety. Red light induces the release of the drug–Ru complex conjugate [Ru(CHLtpy)(biq)(H<sub>2</sub>O)]<sup>2+</sup>. b) Self-assembly of PEG-*b*-P(CPH-*co*-RuCHL) and its phototherapy in hypoxic tumor environment.

in the release of drug–Ru complex conjugate with enhanced anticancer efficiency, which is different from the design of other systems for photoinduced delivery Ru complexes.<sup>[35,41]</sup> CHL–Ru complex conjugates were further grafted to the polymer via the photocleavable Ru–N coordination bond. Red light triggered the cleavage of the CHL–Ru complex conjugates from the polymer chains and subsequent aqution resulted in release of the efficient anticancer CHL–Ru complex conjugate  $[\text{Ru}(\text{CHLtpy})(\text{biq})(\text{H}_2\text{O})]^{2+}$ . The block copolymer PEG-*b*-P(CPH-*co*-RuCHL) self-assembled into micelles, which carried the CHL–Ru complex conjugates to the tumor site and were taken up by hypoxic cancer cells via endocytosis (Figure 1b). Red light passed through skin and tissue and then induced the release of  $[\text{Ru}(\text{CHLtpy})(\text{biq})(\text{H}_2\text{O})]^{2+}$  for PACT. Red-light-responsive PEG-*b*-P(CPH-*co*-RuCHL) is better suited than conventional UV or short-wavelength visible light-responsive polymers for biomedical applications because red light can penetrate deeper into tissue.<sup>[42–47]</sup> We have demonstrated that red light activated Ru complexes with similar responsive wavelengths to PEG-*b*-P(CPH-*co*-RuCHL) after red light passed through tissue with a thickness up to 16 mm.<sup>[48]</sup> Because PEG-*b*-P(CPH-*co*-RuCHL) exhibits improved biocompatibility via PEGylation, enhanced anticancer efficiency via drug conjugation, facilitated endocytosis via micellization, and deep-tissue activation via red light irradiation, PEG-*b*-P(CPH-*co*-RuCHL) is a promising candidate for PACT against hypoxic tumors in vivo.

## 2. Results and Discussion

### 2.1. Synthesis of the Ru-Containing Block Copolymer

PEG-*b*-P(CPH-*co*-RuCHL) was prepared through a multistep route (Figures S1–S3, Supporting Information). The CHL–Ru complex conjugate  $[\text{Ru}(\text{CHLtpy})(\text{biq})(\text{H}_2\text{O})]^{2+}$  was initially synthesized through five steps (Figure S1, Supporting Information). All intermediates and  $[\text{Ru}(\text{CHLtpy})(\text{biq})(\text{H}_2\text{O})]^{2+}$  were fully characterized using nuclear magnetic resonance (NMR) spectroscopy and mass spectrometry (MS) (Figures S4–S11, Supporting Information). Poly(ethylene glycol)-*block*-poly(6-(4-cyanophenoxy) hexyl methacrylate) (PEG-*b*-PCPH) block copolymer was synthesized using poly(ethylene glycol) (PEG) macromolecular chain transfer agent ( $M_n \cong 5 \times 10^3 \text{ g mol}^{-1}$ ) and the monomer 6-(4-cyanophenoxy) hexyl methacrylate (CPH) via reversible addition–fragmentation chain-transfer (RAFT) polymerization (Figure S2, Supporting Information). NMR and gel permeation chromatography (GPC) results demonstrated that the polymer backbone was successfully synthesized (Figures S12–S16, Supporting Information). The molecular weight of the PCPH block was  $1.33 \times 10^4 \text{ g mol}^{-1}$ . Finally, PEG-*b*-P(CPH-*co*-RuCHL) was synthesized by grafting  $[\text{Ru}(\text{CHLtpy})(\text{biq})(\text{H}_2\text{O})]^{2+}$  to PEG-*b*-PCPH through the cyano–Ru coordination (Figure S3, Supporting Information). The chemical structure of PEG-*b*-P(CPH-*co*-RuCHL) was characterized using NMR spectroscopy and Fourier transform infrared (FTIR) spectroscopy (Figures S17 and S18, Supporting Information). <sup>1</sup>H NMR showed that the molecular weight of PEG-*b*-P(CPH-*co*-RuCHL) was  $2.03 \times 10^4 \text{ g mol}^{-1}$ , corresponding to seven CHL–Ru complex conjugates in every polymer chain (Figure S17, Supporting

Information). The weight fraction of the CHL–Ru complex conjugate was  $\approx 45\%$ , which is higher than conventional metallodrug-loaded polymer carriers with less than 10% drug content.<sup>[49,50]</sup> It is well known that increasing drug loading efficiency is a common way to improve therapeutic efficiency. In our case, the weight fraction of CHL–Ru conjugate is as high as  $\approx 45\%$ . Thus, the high-content CHL–Ru complex conjugate in PEG-*b*-P(CPH-*co*-RuCHL) is expected to enhance therapeutic efficiency.

### 2.2. Micelle Preparation and Photoresponsiveness of the Micelles

We prepared block copolymer assemblies by adding water to a THF solution of PEG-*b*-P(CPH-*co*-RuCHL). The micelle solution was collected after removing the organic solvent via dialysis against water. Transmission electron microscopy (TEM) image showed that PEG-*b*-P(CPH-*co*-RuCHL) formed monodisperse micelles with a diameter of  $\approx 15 \text{ nm}$  (Figure 2a and Figure S19, Supporting Information). Dynamic light scattering (DLS) showed that the micelles had a narrow size distribution and the average hydrodynamic diameter of the micelles was 22 nm (Figure 2b). The micelles were well dispersed in water and physiological saline solution. Their size was unchanged even after incubation for 3 d (Figure S20, Supporting Information). These results demonstrated that PEG-*b*-P(CPH-*co*-RuCHL) micelles dispersed well in aqueous solution and had good stability.

The PEG-*b*-P(CPH-*co*-RuCHL) micelles exhibited a broad metal-to-ligand charge transfer (MLCT) band from 400 to 700 nm (Figure 2c and Figure S21, Supporting Information). Excitation of the MLCT band using blue, green, or red light populates the singlet state. Subsequently, an efficient intersystem crossing further populates the triplet state that is thermally activated to a dissociative d–d state, leading to cleavage of the CHL–Ru complex conjugates from PEG-*b*-P(CPH-*co*-RuCHL). To achieve in vivo applications, we used red light in the therapeutic window (650–900 nm) to trigger the photoreaction. Red light irradiation (656 nm) of the micelles red-shifted the MLCT band from 519 nm ( $\lambda_{\text{max}}$  of PEG-*b*-P(CPH-*co*-RuCHL)) to 576 nm ( $\lambda_{\text{max}}$  of  $[\text{Ru}(\text{CHLtpy})(\text{biq})(\text{H}_2\text{O})]^{2+}$ ) (Figure 2c). The detectable spectral change can be achieved less than 0.5 h and the change was identical to that of the photocleavage of similar Ru complexes, suggesting  $[\text{Ru}(\text{CHLtpy})(\text{biq})(\text{H}_2\text{O})]^{2+}$  was cleaved from the polymer.<sup>[48,51]</sup> Additionally, the result from UV–Vis absorption spectroscopy indicated that the photoreaction can be precisely controlled by the irradiation dose (Figure S22a, Supporting Information). The release of  $[\text{Ru}(\text{CHLtpy})(\text{biq})(\text{H}_2\text{O})]^{2+}$  with different irradiation doses was quantified using inductively coupled plasma mass spectrometry (ICP-MS) (Figure 2d). Up to 84% of  $[\text{Ru}(\text{CHLtpy})(\text{biq})(\text{H}_2\text{O})]^{2+}$  was released under light irradiation in our experimental condition. In comparison, only  $\approx 7\%$  of  $[\text{Ru}(\text{CHLtpy})(\text{biq})(\text{H}_2\text{O})]^{2+}$  was released in the dark after 24 h, suggesting the good stability of the micelles during long time incubation (Figure S23, Supporting Information).

### 2.3. Cell Toxicity of the Drug–Ru Complex Conjugate

The released  $[\text{Ru}(\text{CHLtpy})(\text{biq})(\text{H}_2\text{O})]^{2+}$  is a conjugate of a Ru complex and a commercial anticancer drug CHL, both of



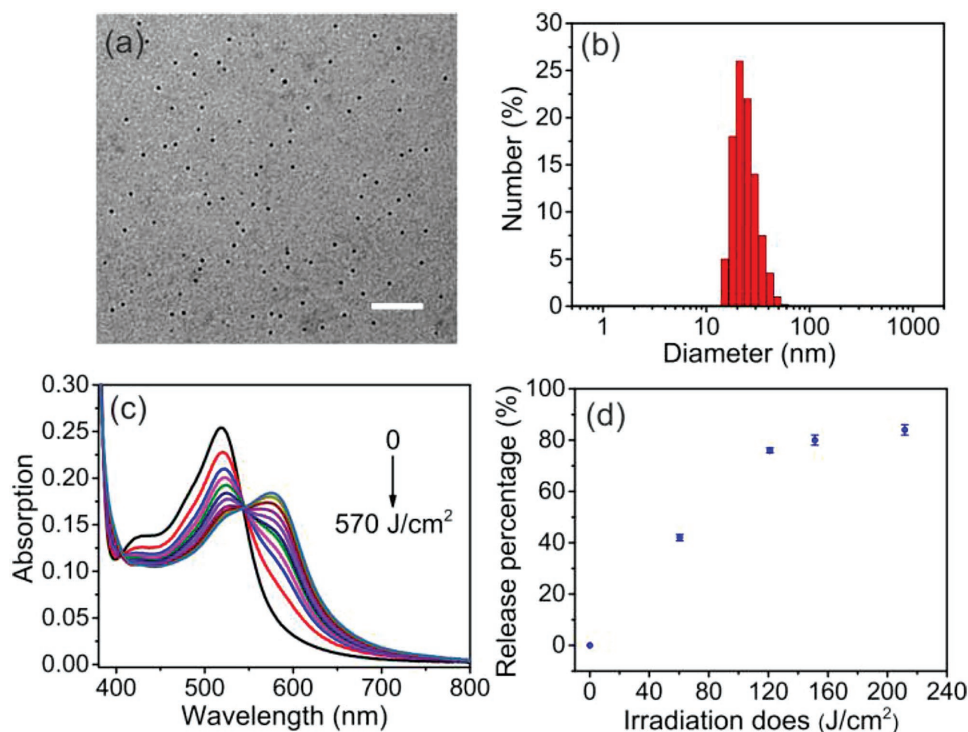


**Figure 2.** a) TEM image of PEG-*b*-P(CPH-*co*-RuCHL) micelles. Scale bar: 150 nm. b) The diameter of the micelles measured using dynamic light scattering. c) UV-vis spectra of the micelles after 656 nm light irradiation in a cell culture medium. Light intensity: 26.5 mW cm<sup>-2</sup>, irradiation time: 0, 0.5, 1.0, 1.5, 2.0, 2.5, 3.0, 3.5, 4.0, 5.0, and 6.0 h. d) The release percentage of [Ru(CHLtpy)(biq)(H<sub>2</sub>O)]<sup>2+</sup> from PEG-*b*-P(CPH-*co*-RuCHL) under red light irradiation (656 nm).

which can inhibit cancer cell growth. Thus, [Ru(CHLtpy)(biq)(H<sub>2</sub>O)]<sup>2+</sup> is expected to be an efficient anticancer agent. The cytotoxicity of [Ru(CHLtpy)(biq)(H<sub>2</sub>O)]<sup>2+</sup> was tested using HeLa cells, a commonly used model cancer cell line for evaluating anticancer activities of new anticancer materials (Figure 3a). HeLa cells were incubated with [Ru(CHLtpy)(biq)(H<sub>2</sub>O)](PF<sub>6</sub>)<sub>2</sub> with a concentration from 1.25 to 50 μg mL<sup>-1</sup> for 24 h. Cell viability decreased as the concentration of [Ru(CHLtpy)(biq)(H<sub>2</sub>O)]<sup>2+</sup> increased. The half maximal effective concentration (EC<sub>50</sub>) of [Ru(CHLtpy)(biq)(H<sub>2</sub>O)]<sup>2+</sup> to HeLa cells was ≈13.7 μg mL<sup>-1</sup>, much lower than those of both [Ru(CHLtpy)(biq)(H<sub>2</sub>O)]<sup>2+</sup> (≈30 μg mL<sup>-1</sup>, Figure S24, Supporting Information) and CHL (≈150 μg mL<sup>-1</sup>).<sup>[52]</sup> The result indicated that the two anticancer moieties had synergistic effects and the conjugate [Ru(CHLtpy)(biq)(H<sub>2</sub>O)]<sup>2+</sup> had improved cytotoxicity toward cancer cells. The cytotoxicity of the complex after red light irradiation (671 nm, 120 J cm<sup>-2</sup>) was also studied (Figure 3a). The EC<sub>50</sub> value for HeLa cells after irradiation was ≈10.3 μg mL<sup>-1</sup>, which is close to that without irradiation. EC<sub>50</sub> values under dark and light irradiation were similar because no <sup>1</sup>O<sub>2</sub> was generated when [Ru(CHLtpy)(biq)(H<sub>2</sub>O)]<sup>2+</sup> was irradiated with light (Figure 3b).

## 2.4. Cellular Uptake and Cytotoxicity Assessment

Encouraged by the improved anticancer efficiency of [Ru(CHLtpy)(biq)(H<sub>2</sub>O)]<sup>2+</sup> compared to CHL and [Ru(tpy)(biq)(H<sub>2</sub>O)]<sup>2+</sup>, we used PEG-*b*-P(CPH-*co*-RuCHL) micelles as nanocarriers for PACT. First, we studied cellular uptake

of PEG-*b*-P(CPH-*co*-RuCHL) micelles (Figure 4a). A hydrophobic dye was loaded into the core of the micelles during self-assembly for fluorescence tracing. We verified if the loaded dye leaked out by monitoring fluorescence after dialysis of the micelles (Figures S25 and S26, Supporting Information). No fluorescence was detected after dialysis of the micelle dispersion, suggesting no leakage of the dye from the micelles. The micelles loaded with the dye were incubated with HeLa cells in the dark for 6 h. Subsequently, the cells were washed thoroughly and cell nuclei were stained with Hoechst 33342. Confocal laser scanning microscopy (CLSM) revealed green fluorescence from the micelles in the cytoplasm, indicating the micelles were taken up by the cancer cells (Figure 4a, top). We also imaged the cells without incubation with the micelles as a control experiment (Figure 4a, bottom). No green fluorescence was observed, suggesting the observed green fluorescence (Figure 4a, top) was from the micelles.

The cytotoxicity of PEG-*b*-P(CPH-*co*-RuCHL) micelles in the dark and after light irradiation was also studied (Figure 4b). In the dark, the micelles showed negligible toxic to HeLa cells, suggesting the micelles had good biocompatibility. In contrast, irradiating (656 nm, 60 J cm<sup>-2</sup>) cancer cells incubated with PEG-*b*-P(CPH-*co*-RuCHL) micelles significantly decreased the cell viability (Figure 4b). The EC<sub>50</sub> of polymeric micelles was less than 25 μg mL<sup>-1</sup>, which is much lower than that of CHL (150 μg mL<sup>-1</sup>).<sup>[52]</sup> Because light irradiation (656 nm, 60 J cm<sup>-2</sup>) on the micelles (100 μL, 200 μg mL<sup>-1</sup>) resulted in 90% conversion of the photoreaction (Figure S20b, Supporting Information), we interpret that the released [Ru(CHLtpy)(biq)

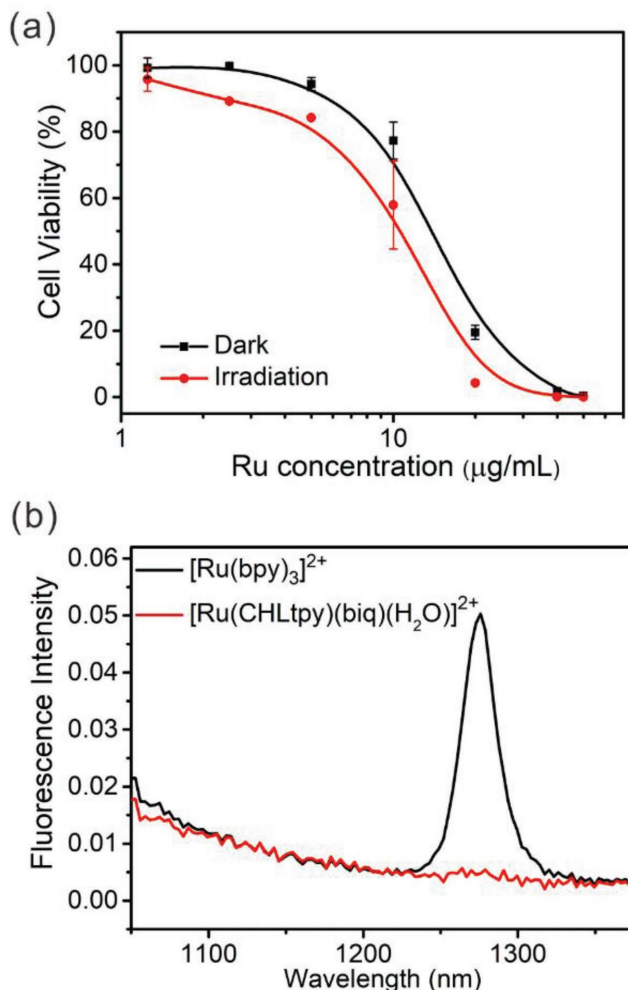


**Figure 3.** a) Viability of HeLa cells incubated with  $[\text{Ru}(\text{CHLtpy})(\text{biq})(\text{H}_2\text{O})](\text{PF}_6)_2$  with various concentrations for 24 h. HeLa cells were kept in the dark or under light irradiation ( $671 \text{ nm}$ ,  $120 \text{ J cm}^{-2}$ ) at the beginning of the incubation. b) Emission spectra of  $^1\text{O}_2$  ( $\lambda_{\text{em}} = 1275 \text{ nm}$ ) generated in the solutions of  $[\text{Ru}(\text{CHLtpy})(\text{biq})(\text{H}_2\text{O})](\text{PF}_6)_2$  and  $[\text{Ru}(\text{bpy})_3]\text{Cl}_2$  in  $\text{CD}_3\text{OD}$  after excitation at  $\lambda_{\text{ex}} = 450 \text{ nm}$ .  $A_{450 \text{ nm}} = 0.1$  (4 mm path length) for all samples.  $[\text{Ru}(\text{bpy})_3]\text{Cl}_2$  was used as a reference sample ( $\Phi\Delta = 0.73$  in  $\text{CD}_3\text{OD}$ ).<sup>[53]</sup>

$(\text{H}_2\text{O})^{2+}$  from the micelles inhibited cancer cell growth. As a comparison, cytotoxicity of PEG-*b*-PCPH micelles without the drug–Ru complex conjugate was also tested. The PEG-*b*-CPH polymer micelles showed no toxicity both in the dark and under light irradiation (Figure S27, Supporting Information), which further proved that light-enhanced toxicity arose from the release of the drug–Ru complex conjugates.

In the next step, we compared cytotoxicity of PEG-*b*-P(CPH-*co*-RuCHL) micelles under normoxic and hypoxic conditions (Figure 4c). For the hypoxic group, cells were incubated in the culture medium containing  $\text{CoCl}_2$  ( $100 \times 10^{-6} \text{ M}$ ), which was used as the hypoxia inducer.<sup>[28]</sup> HeLa cells under normoxic conditions were also prepared simultaneously. Then, the cells were incubated with micelles ( $25 \mu\text{g mL}^{-1}$ ) for 6 h prior to red light irradiation. In both normoxic and hypoxic conditions, only irradiating cancer cells ( $671 \text{ nm}$ ,  $120 \text{ J cm}^{-2}$ ) (orange bars) or

only incubating cancer cells with micelles ( $25 \mu\text{g mL}^{-1}$ ) (green bars) cannot efficiently kill the cancer cells. Light irradiation in the presence of the micelles decreased the cell viability to 44.9% in the hypoxic condition and 45.1% in the normoxic condition (red bars). The results showed that the phototoxicity of the micelles was independent of oxygen level. Actually, PEG-*b*-P(CPH-*co*-RuCHL) cannot generate  $^1\text{O}_2$  under light irradiation (Figure S28, Supporting Information), suggesting that the inhibition of cancer cell growth was not due to  $^1\text{O}_2$  generation but because of the released  $[\text{Ru}(\text{CHLtpy})(\text{biq})(\text{H}_2\text{O})]^{2+}$ .

## 2.5. In Vivo Anticancer Assessment

The  $\text{O}_2$ -independent phototoxicity of PEG-*b*-P(CPH-*co*-RuCHL) micelles in vitro motivated us to investigate PACT using the micelles in vivo (Figure 5a). HeLa tumor-bearing mice were treated with saline (Control group), light only (Light group), PEG-*b*-P(CPH-*co*-RuCHL) micelles only (Micelles group), and PEG-*b*-P(CPH-*co*-RuCHL) micelles with light (Micelles + Light group). The micelles or saline were injected into the central part of solid tumors, which were hypoxic.<sup>[54]</sup> After injection for 4 h (Micelles + Light group), the tumors were irradiated with red light ( $360 \text{ J cm}^{-2}$ ). The light irradiation for the in vivo anticancer assessment was comparable to that of the in vitro experiment ( $120 \text{ J cm}^{-2}$ ) because the light power was reduced to one third in the in vivo experiment (Figure S29, Supporting Information). Besides, light irradiation did not cause overheating problem and is thus suitable for phototherapy in the mouse model (Figure S30, Supporting Information). We assessed the anticancer effects of each group by monitoring the tumor volumes over 14 d (Figure 5b). The relative tumor volume ( $V_t/V_0$ ) in the Micelles + Light group was below 1 after the treatment, showing that the tumor growth was efficiently inhibited. In contrast, the relative tumor volumes in the other three groups were three to four times larger after the treatments for 14 d. These results were also represented using the photographs of the experimental mice after different treatments (Figure 5c). Additionally, the histological analysis of the tumor tissues was carried out to evaluate the antitumor efficacy of different treatments (Figure 5d). The hematoxylin and eosin (H&E) staining assay showed that most tumor cells were severely damaged in the mice treated by micelles with irradiation (Micelles + Light group). However, most cancer cells were still alive in the other three groups. The excellent antitumor efficiency in hypoxic tumors is because PEG-*b*-P(CPH-*co*-RuCHL) micelles exhibit  $\text{O}_2$ -independent phototoxicity via light-triggered release of the anticancer drug–Ru complex conjugate.

The body weight of the mice was monitored during the treatment (Figure S31, Supporting Information). Almost no change of the body weight was observed in all groups, indicating that the injection of PEG-*b*-P(CPH-*co*-RuCHL) micelles and irradiation with light demonstrated minimal side effects on mice. In addition, the micelles did not cause any hemolysis due to the excellent compatibility of PEG-*b*-P(CPH-*co*-RuCHL) micelles to red blood cells (Figure S32, Supporting Information). To further access the in vivo safety of PEG-*b*-P(CPH-*co*-RuCHL), the histological analysis of major organs including heart, liver, spleen, lung, and kidney was carried out (Figure 5e). No

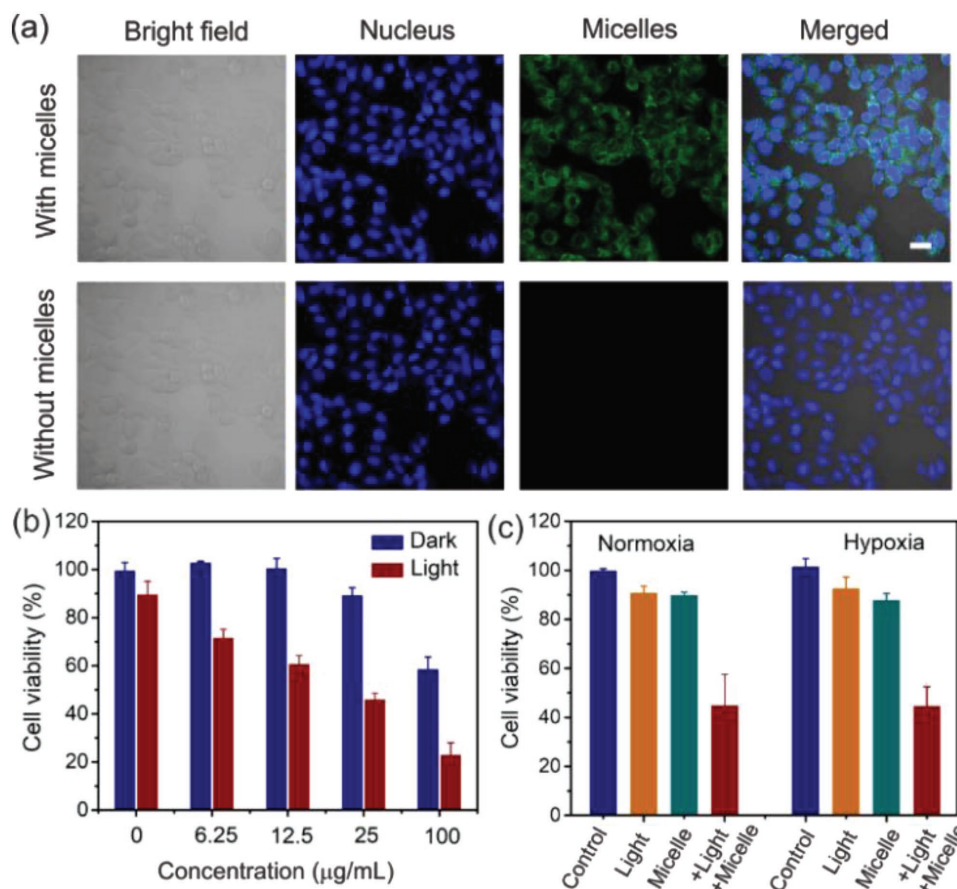


**Figure 4.** a) Confocal laser scanning microscopy images of HeLa cells incubated with or without PEG-*b*-P(CPH-*co*-RuCHL) micelles. Nuclei were stained with Hoechst 33342 (blue). Scale bar: 20 µm. b) Viability of HeLa cells incubated with different concentrations of the micelles in the dark and after irradiation (656 nm, 60 J cm<sup>-2</sup>). The cells were irradiated with red light (656 nm, 60 J cm<sup>-2</sup>) after incubation with the micelles for 6 h. Cell viability was tested after the cells were further incubated for 24 h. c) Viability of HeLa cells after different treatments in normoxic and hypoxic conditions. Cells without any treatment were set as the Control group; Cells only irradiated with red light (671 nm, 120 J cm<sup>-2</sup>) were set as Light group; Cells only incubated with micelles were set as Micelle group; Cells irradiated with red light (671 nm, 120 J cm<sup>-2</sup>) after incubation with the micelles (25 µg mL<sup>-1</sup>) for 6 h were set as Micelle + Light group. Cell viability was tested after incubating the cells for 24 h.

damage or change to physiological morphology was found in organ slices from H&E staining images in the Micelles + Light group, confirming that PACT using PEG-*b*-P(CPH-*co*-RuCHL) micelles eliminated substantial systemic toxicity in living animals. The H&E staining experiments indicated that the toxicity of PEG-*b*-P(CPH-*co*-RuCHL) micelles can be precisely activated via light irradiation.

### 3. Conclusion

We reported the design of a Ru-containing amphiphilic polymer for PACT in vivo. The Ru-containing polymer, PEG-*b*-P(CPH-*co*-RuCHL), contains novel red-light-cleavable drug-Ru conjugates. The drug-Ru complex conjugates bearing a very high content (≈45 wt%) in the polymer were carried by the polymer and can be released on-demand via red light irradiation. The Ru-containing polymer self-assembled into micelles and internalized into tumor cells. Light irradiation induced the release of drug-Ru complex conjugates, which inhibited tumor cell growth. Because the photoinduced drug release process is

oxygen-independent, the polymer micelles are suited for PACT against tumor cells with hypoxic environments. The polymer micelles were further used for PACT in a tumor-bearing mouse model, which completely inhibited tumor growth. Moreover, the treatment using the polymer micelles eliminated substantial systemic toxicity in living animals. PACT based on our metal-polymers with red-light-cleavable drug-Ru complex conjugates is a new strategy to overcome the problem of conventional PDT in hypoxic environments. The development of polymers with drug-Ru complex conjugates opens up an avenue for the design of polymeric therapeutics for PACT against hypoxic tumors.

### 4. Experimental Section

**Preparation of PEG-*b*-P(CPH-*co*-RuCHL) Micelles:** PEG-*b*-P(CPH-*co*-RuCHL) micelles were prepared through adding water to organic solution of the polymer. Briefly, PEG-*b*-P(CPH-*co*-RuCHL) (1 mg) was dissolved in THF (100 µL) and stirred for 20 min. 2 mL Milli-Q water was added to the THF solution containing polymers dropwise, and the solution was kept stirring for another 20 min. The micelle solution was then dialyzed against water for 48 h to remove THF through a dialysis tube.



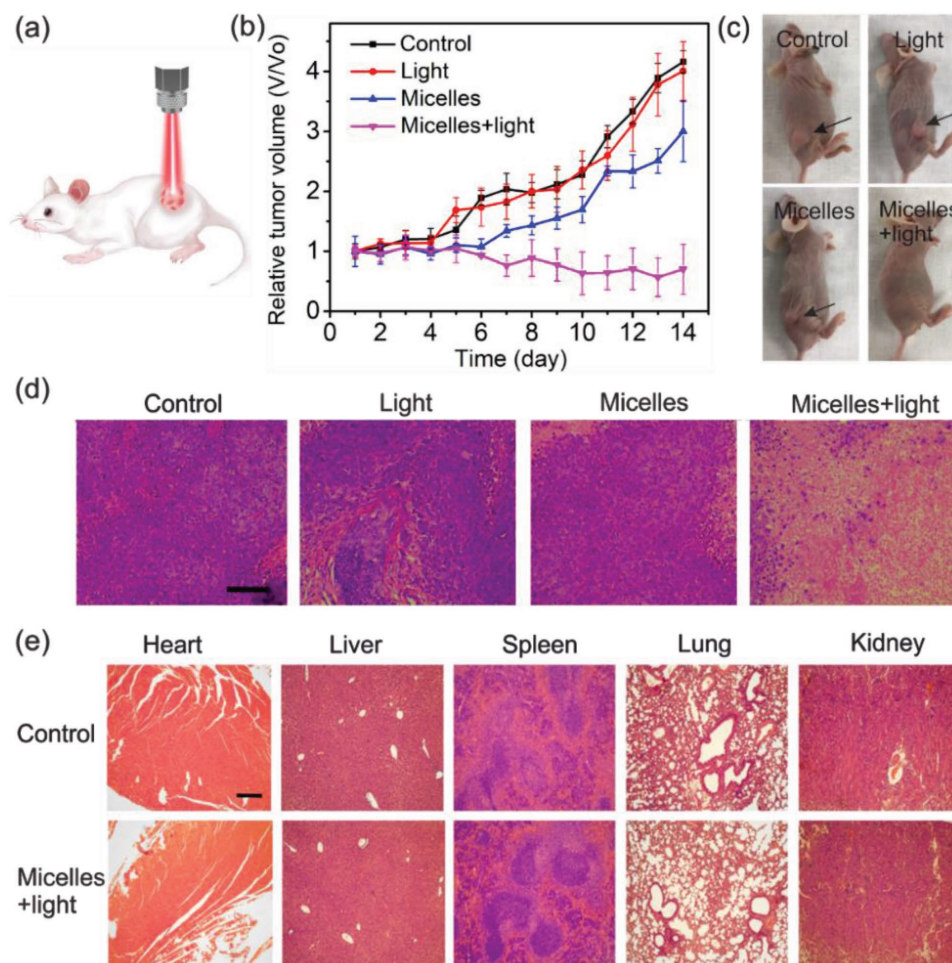


**Figure 5.** a) Schematic illustration of anticancer phototherapy using PEG-*b*-P(CPH-*co*-RuCHL) micelles in a tumor-bearing mouse model. Red light activates the micelles at the tumor site. b) Relative tumor volume of each group during treatments,  $n = 5$ . c) Photos of the tumor-bearing mice after different treatments. The tumors were indicated using the black arrows. d) H&E staining images of the tumors of the Control and the Micelles + Light groups at Day 14. Scale bar: 100  $\mu\text{m}$ . e) H&E staining images of major organs from the Control and the Micelles + Light groups after treatments. Scale bar: 100  $\mu\text{m}$ .

**Preparation of Fluorescent Dye Loaded PEG-*b*-P(CPH-*co*-RuCHL) Micelles:** To prepare dye-loaded PEG-*b*-P(CPH-*co*-RuCHL) micelles, coumarin-6 solution (200  $\mu\text{g mL}^{-1}$  in DMF, 10  $\mu\text{L}$ ) was added to the solution of PEG-*b*-P(CPH-*co*-RuCHL) in THF (10  $\text{mg mL}^{-1}$ , 100  $\mu\text{L}$ ), and stirred for 1 h. 2 mL Milli-Q water was added to the THF solution containing polymers dropwise, and the solution was kept stirring for another 20 min. The micelle solution was then dialyzed against water for 48 h to remove THF through a dialysis tube.

**Cell Viability:** To study the cytotoxicity of the Ru complex or micelles, HeLa cells suspended in DMEM were seeded in 96-well plates at a density of 6400 cells per well for 2 d. The cells were incubated with various concentrations of Ru complex from 1.25–50  $\mu\text{g mL}^{-1}$  for 4 h before irradiation or with various concentrations of micelles from 6.25 to 150  $\mu\text{g mL}^{-1}$  for 6 h before irradiation. To investigate the toxic effect of micelles under hypoxia, the cells were prepared as described above except for using the medium containing  $100 \times 10^{-6}$  M of cobalt chloride ( $\text{CoCl}_2$ ) to switch on hypoxic cellular response for 24 h. Then, the cells were treated with 25  $\mu\text{g mL}^{-1}$  of micelles for 6 h before irradiation. After exposed to the light, the cells were incubated at 37  $^\circ\text{C}$  for 24 h in an incubator. Samples without being treated with light were covered with a piece of Al foil and performed in parallel. Cells without any treatment were calculated as 100% cell viability and set as the negative control. 20% DMSO incubated samples were used as a vehicle control. Cell

viability was evaluated using the CellTiter-Glo luminescent cell viability assay (Promega, USA) according to the manufacturer's protocol. The method is on the basis of amount of ATP, reflecting the amount of active cells metabolically. The luminescence was tested 10 min after incubation with the agent through a plate reader (Infinite M1000, Tecan, Germany).

**Cell Imaging by Confocal Laser Scanning Microscopy:** For cellular uptake study, HeLa cells were seeded at a density of  $2 \times 10^4$  cells per well in a Nunc Lab-Tek 8 well plate (Thermo Fisher, USA) and cultured for 24 h in DMEM complete medium. After attached to the well, the cells were incubated with fresh medium containing dye-loaded micelles (50  $\mu\text{g mL}^{-1}$ ) for another 6 h. After that, the cells were washed twice with PBS, stained with Hoechst 33342 and were observed with a Zeiss LSM 760 system (Zeiss, Germany). The parameters used for the CLSM studies were described as follows: Dye-loaded micelles were excited with a laser (458 nm), detected at 470–555 nm and pseudocolored in green. The cell nucleus was stained with Hoechst 33342 ( $1 \times 10^{-6}$  M, Life technologies, USA), excited with a laser (405 nm), detected at 410–470 nm and pseudocolored in blue. The CLSM images are shown in Figure 4a.

**Hemolysis Assay:** 0.6 mL fresh blood was obtained from the nude mice and suspended in 10 mL saline. Red blood cells (RBCs) were collected through centrifugation at 2000 rpm for 4–5 min. The cell solution was washed with saline for several times until red color can be seen from the supernatant. RBCs were suspended in 6 mL saline.



0.2 mL RBCs suspension was added to 0.8 mL saline containing different concentrations of micelles to offer the final concentrations of 50, 250, 500, and 750  $\mu\text{g mL}^{-1}$ . The 0.2 mL RBCs suspension incubated with 0.8 mL saline or 0.8 mL water was used as negative control and positive control. The solution was gently mixed, left at 37 °C for 4 h. The red blood cells were collected via centrifugation at 2000 rpm, and the absorbance value (570 nm) of the supernatant was measured. The hemolysis percentage was calculated according to the reported method.<sup>[35]</sup>

**In Vivo Thermal Imaging:** All protocols for animal studies conformed to the Guide for the Care and Use of Laboratory Animals. All animal experiments were performed in accordance with guidelines approved by the ethics committee of Peking University. The Balb/c nude mouse bearing HeLa tumor exposed to a 660 nm laser irradiation, thermal images of mice were continuously obtained using an infrared thermal camera which was used to monitor temperature changes at the tumor site. No visible photothermal effect was observed during the treatment.

**In Vivo Therapeutic Efficacy:** The tumor-bearing mouse model was established by subcutaneous injection of  $5 \times 10^6$  HeLa cells into a mouse. Two weeks after implantation, the tumor-bearing mice were randomly divided into four groups: 1) mice without any treatment as the control group; 2) mice only exposed to 660 nm light irradiation ( $360 \text{ J cm}^{-2}$ ); 3) mice injected with micelles ( $500 \mu\text{g mL}^{-1}$ ) without irradiation; 4) mice injected with micelles ( $500 \mu\text{g mL}^{-1}$ ) and then exposed to 660 nm light irradiation ( $360 \text{ J cm}^{-2}$ ). Mice were treated with the micelles ( $500 \mu\text{g mL}^{-1}$ ) by injecting the micelles to the central part of the tumor at day 1, day 3, and day 5. After 4 h, the mice in groups (2) and (4) were locally irradiated with 660 nm laser. The relative tumor volumes ( $v/v_0$ ,  $v_0$  is tumor volume of pre therapy) were calculated to evaluate the therapy efficiency. And the relative body weights ( $m/m_0$ ,  $m_0$  is the body weight of pre therapy) were calculated to evaluate toxicity during the treatment.

**H&E Staining:** After treatment, mice were sacrificed, tumors and important organs, including heart, livers, spleen, lung, kidney, and tumors were harvested and collected for H&E histology analysis. The H&E staining of tumors and these organs were carried out by Beijing Lawke Health Laboratory Center for Clinical Laboratory Development. The images were acquired by a fluorescence microscope (EVOS XL Core, Life technologies, USA).

## Supporting Information

Supporting Information is available from the Wiley Online Library or from the author.

## Acknowledgements

W.S., Y.W., and R.T. contributed equally to this work. This work was supported by the Deutsche Forschungsgemeinschaft (DFG, WU 787/2-1 and WU 787/8-1), the Fonds der Chemischen Industrie (FCI, No. 661548), the Fundamental Research Funds for the Central Universities (2018011013), and NSFC-DFG (31761133013), and the Thousand Talents Plan. The authors thank G. Kircher and A. Best for their technical support. NWO (The Netherlands Organization for Scientific Research) is acknowledged for a VIDI grant to S.B. The affiliations and the funding statement were updated on September 26, 2018, following initial publication on early view.

## Conflict of Interest

The authors declare no conflict of interest.

## Keywords

hypoxic tumors, metallopolymers, phototherapy, red light, ruthenium

Received: June 19, 2018

Revised: July 16, 2018

Published online: August 14, 2018

- [1] I. Romero-Canelón, P. J. Sadler, *Inorg. Chem.* **2013**, *52*, 12276.
- [2] C. Mari, V. Pierroz, S. Ferrari, G. Gasser, *Chem. Sci.* **2015**, *6*, 2660.
- [3] K. Vellaisamy, G. Li, C.-N. Ko, H.-J. Zhong, S. Fatima, H.-Y. Kwan, C.-Y. Wong, W.-J. Kwong, W. Tan, C.-H. Leung, D.-L. Ma, *Chem. Sci.* **2018**, *9*, 1119.
- [4] K. M. Boyle, J. K. Barton, *J. Am. Chem. Soc.* **2018**, *140*, 5612.
- [5] G. Yu, M. Zhang, M. L. Saha, Z. M. L. Saha, Z. Mao, J. Chen, Y. Yao, Z. Zhou, Y. Liu, C. Gao, F. Huang, X. Chen, P. J. Stang, *J. Am. Chem. Soc.* **2017**, *139*, 15940.
- [6] C. S. Burke, A. Byrne, T. E. Keyes, *J. Am. Chem. Soc.* **2018**, *140*, 6945.
- [7] J. D. Knoll, C. Turro, *Coord. Chem. Rev.* **2015**, *6*, 2660.
- [8] B. A. Albani, B. Pena, N. A. Leed, N. A. B. G. de Paula, C. Pavani, M. S. Baptista, K. R. Dunbar, C. Turro, *J. Am. Chem. Soc.* **2014**, *136*, 17095.
- [9] H. Huang, B. Yu, P. Zhang, J. Huang, Y. Chen, G. Gasser, L. Ji, H. Chao, *Angew. Chem., Int. Ed.* **2015**, *54*, 14049.
- [10] N. W. Choi, S. S. Verbridge, R. M. Williams, J. Chen, J.-Y. Kim, R. Schmehl, C. E. Farnum, W. R. Zipfel, C. Fischbach, A. D. Stroock, *Biomaterials* **2012**, *33*, 2710.
- [11] T. Sainuddin, J. McCain, M. Pinto, H. Yin, J. Gibson, M. Hetu, S. A. McFarland, *Inorg. Chem.* **2016**, *55*, 83.
- [12] L. Kohler, L. Nease, P. Vo, J. Garofolo, D. K. Heidary, R. P. Thummel, E. C. Glazer, *Inorg. Chem.* **2017**, *56*, 12214.
- [13] M. Wenzel, A. de Almeida, E. Bigaeva, P. Kavanagh, M. Picquet, P. L. Gendre, E. Bodio, A. Casini, *Inorg. Chem.* **2016**, *55*, 2544.
- [14] C. Griffith, A. S. Dayoub, T. Jaranatne, N. Alatrash, A. Mohamedi, K. Abayan, Z. S. Breitbach, D. W. Armstrong, F. M. MacDonnell, *Chem. Sci.* **2017**, *8*, 3726.
- [15] M. R. Gill, P. J. Jarman, S. Halder, M. G. Walker, H. K. Saeed, J. A. Thomas, C. Smythe, K. Ramadan, K. A. Vallis, *Chem. Sci.* **2018**, *9*, 841.
- [16] M. Dickerson, B. Howerton, Y. Bae, E. C. Glazer, *J. Mater. Chem. B* **2016**, *4*, 394.
- [17] E. Wachter, D. K. Heidary, B. S. Howerton, S. Parkin, E. C. Glazer, *Chem. Commun.* **2012**, *48*, 9649.
- [18] B. S. Howerton, D. K. Heidary, E. C. Glazer, *J. Am. Chem. Soc.* **2012**, *134*, 8324.
- [19] M. A. Sgambellone, A. David, R. N. Garner, K. R. Dunbar, C. Turro, *J. Am. Chem. Soc.* **2013**, *135*, 11274.
- [20] L. N. Lameijer, D. Ernst, S. L. Hopkins, M. S. Meijer, S. H. C. Askes, S. E. Le Devedec, S. Bonnet, *Angew. Chem., Int. Ed.* **2017**, *56*, 11549.
- [21] V. H. S. van Rixel, B. Siewert, S. L. Hopkins, S. H. C. Askes, A. Busemann, M. A. Siegler, S. Bonnet, *Chem. Sci.* **2016**, *7*, 4922.
- [22] J. K. White, R. H. Schmehl, C. Turro, *Inorg. Chim. Acta* **2017**, *454*, 7.
- [23] N. Karaoun, A. K. Renfrew, *Chem. Commun.* **2015**, *51*, 14038.
- [24] A. N. Hidayatullah, E. Wachter, D. K. Heidary, S. Parkin, E. C. Glazer, *Inorg. Chem.* **2014**, *53*, 10030.
- [25] E. Wachter, D. Moyá, S. Parkin, E. C. Glazer, *Inorg. Chem.* **2011**, *50*, 9045.
- [26] K. Liu, R. Xing, Q. Zou, G. Ma, H. Mohwald, X. Yan, *Angew. Chem., Int. Ed.* **2016**, *55*, 3036.
- [27] S. S. Lucky, K. C. Soo, Y. Zhang, *Chem. Rev.* **2015**, *115*, 1990.

- [28] S. Shen, C. Zhu, D. Huo, M. Yang, J. Xue, Y. Xia, *Angew. Chem., Int. Ed.* **2017**, *56*, 8801.
- [29] B. A. Albani, C. B. Durr, C. Turro, *J. Phys. Chem. A* **2013**, *117*, 13885.
- [30] R. Araya, V. Andino-Pavlovsky, R. Yuste, R. Etchenique, *ACS Chem. Neurosci.* **2013**, *4*, 1163.
- [31] V. Nikolenko, R. Yuste, L. Zayat, L. M. Baraldo, R. Etchenique, *Chem. Commun.* **2005**, 1752.
- [32] M. Huisman, J. K. White, V. G. Lewalski, I. Podgorski, C. Turro, J. M. Kodanko, *Chem. Commun.* **2016**, *52*, 12590.
- [33] W. Sun, X. Zeng, S. Wu, *Dalton Trans.* **2017**, *47*, 283.
- [34] W. Sun, M. Parowatkin, W. Steffen, H. J. Butt, V. Mailänder, S. Wu, *Adv. Healthcare Mater.* **2016**, *5*, 467.
- [35] W. Sun, S. Li, B. Haupler, J. Liu, S. Jin, W. Steffen, U. S. Schubert, H. J. Butt, X.-J. Liang, S. Wu, *Adv. Mater.* **2017**, *29*, 1603702.
- [36] N. Lameijer, T. G. Brevé, V. H. S. van Rixel, S. H. C. Askes, M. A. Siegler, S. Bonnet, *Chem. Eur. J.* **2018**, *24*, 2709.
- [37] L. M. Loftus, J. K. White, B. A. Albani, L. Kohler, J. J. Kodanko, R. P. Thummel, K. R. Dunbar, C. Turro, *Chem. Eur. J.* **2016**, *22*, 3704.
- [38] Y. Zhang, H. F. Chan, K. W. Leong, *Adv. Drug Delivery Rev.* **2013**, *65*, 104.
- [39] P. M. Kelly, C. Åberg, E. Polo, A. O'Connell, J. Cookman, J. Fallon, Z. Krpeti, K. A. Dawson, *Nat. Nanotechnol.* **2015**, *10*, 472.
- [40] F. Bertoli, D. Garry, M. P. Monopoli, A. Salvati, K. A. Dawson, *ACS Nano* **2016**, *10*, 10471.
- [41] G. Boeuf, G. V. Roullin, J. Moreau, L. V. Gulick, N. Z. Pineda, C. Terry, D. Ploton, M. C. Andry, F. Chuburu, S. Dukic, M. Molinari, G. Lemerrier, *ChemPlusChem* **2014**, *79*, 171.
- [42] M. Abbas, Q. Zou, S. Li, X. Yan, *Adv. Mater.* **2017**, *29*, 1605021.
- [43] J. F. Gohy, Y. Zhao, *Chem. Soc. Rev.* **2013**, *42*, 7117.
- [44] K. Hildebrandt, K. Elies, D. R. D'hooge D, J. P. Blinco, C. Barner-Kowollik, *J. Am. Chem. Soc.* **2016**, *138*, 7048.
- [45] Y. Zhao, *Macromolecules* **2012**, *45*, 3647.
- [46] J. P. Menzel, B. B. Noble, A. Lauer, M. L. Coote, J. P. Blinco, C. Barner-Kowollik, *J. Am. Chem. Soc.* **2017**, *139*, 15812.
- [47] C. H. Quek, K. W. Leong, *Nanomaterials* **2012**, *2*, 92.
- [48] W. Sun, R. Thiramanas, L. D. Slep, X. Zeng, V. Mailänder, S. Wu, *Chem. Eur. J.* **2017**, *23*, 10832.
- [49] J. Yang, W. Liu, M. Sui, J. Tang, Y. Shen, *Biomaterials* **2011**, *32*, 9136.
- [50] S. Aryal, C.-M. J. Hu, L. Zhang, *ACS Nano* **2010**, *4*, 251.
- [51] L. Zayat, M. G. Noval, J. Campi, C. I. Calero, D. J. Calvo, R. Etchenique, *ChemBioChem* **2007**, *8*, 2035.
- [52] I. S. Vijayashree, P. Niranjana, G. Prabhu, V. V. Sureshbabu, J. Manjanna, *J. Cluster Sci.* **2017**, *28*, 133.
- [53] J.-A. Cuello-Garibo, M. S. Meijer, S. Bonnet, *Chem. Commun.* **2017**, *53*, 6768.
- [54] J. M. Brown, W. R. Wilson, *Nat. Rev. Cancer* **2004**, *4*, 437.